Resistivity, magnetoresistance and field-dependent AC susceptibility of ErNiBC



1996 J. Phys.: Condens. Matter 8 L483

(http://iopscience.iop.org/0953-8984/8/35/001)

J. Phys.: Condens. Matter **8** (1996) L483–L490. Printed in the UK

**LETTER TO THE EDITOR**

# Resistivity, magnetoresistance and field-dependent AC susceptibility of ErNiBC

X Z Zhou, H P Kunkel and Gwyn Williams

Department of Physics, University of Manitoba, Winnipeg, R3T 2N2, Canada

Received 11 June 1996

**Abstract.** Measurements are reported on the temperature and field dependence of the resistivity of ErNiBC between 1.5 and 15 K in fields up to 7 T. The zero-field resistivity displays an abrupt fall below 4.1 K and an overall character consistent with ferromagnetic ordering, as inferred from recent neutron scattering measurements; the data below 2 K can be reproduced by a model describing conduction-electron scattering by spin waves following a gapped dispersion relation: $E_q = \Delta + Dq^2$, with the gap parameter $\Delta = 2 \pm 0.5$ K. Data acquired in various fixed fields can be adequately reproduced by adding a conventional Zeeman term to $\Delta$. The field-dependent AC susceptibility does not display features normally associated with critical fluctuations at a ferromagnetic transition, although here the latter might be obscured by a substantial regular contribution, the presence of which could signify considerable magnetic anisotropy most likely to be associated with single ion spin–orbit coupling at Er sites.

Compounds of the type $RNi_2B_2C$ (R = Y or rare earth) have been the subject of considerable experimental and theoretical interest over the past two years. This interest was generated initially by the observation of superconductivity in systems with R = Lu and Y at relatively high temperatures $T_c \simeq 15$ to 16.5 K [1]) and the possible mechanisms responsible for such effects (higher phonon frequencies expected from low mass boron/carbon atoms, localized spin fluctuations around Ni sites, etc). However, recent reports of various types of magnetically ordered ground states in compounds formed when R is taken from the second half of the rare-earth series [2]—particularly the observation of an incommensurate antiferromagnetic structure in $ErNi_2B_2C$ and $HoNi_2B_2C$ [3]—have resulted in much recent effort being directed towards understanding the magnetic properties of these compounds, and the interplay between magnetism and superconductivity in them.

These compounds belong to a broader class of systems described by a more general formula $(RC)_n(NiB)_m$, with $m$ and $n$ integers, in which—broadly speaking—modifications are made to the $Ni_2$–$B_2$ layering by variations in frequency of intercalating R–C layers. Indeed, while intrasheet interactions between magnetic rare-earth atoms appear to be of predominantly ferromagnetic character, changes in the interplane coupling induced by small variations in the $c$-axis spacing appear pivotal in determining the overall ground state spin configuration. Striking examples of these latter effects appear in recent reports of neutron scattering in ErNiBC and HoNiBC [4] which conclude that the former undergoes ferromagnetic ordering near 4 K while the latter displays a ferromagnetic sheet structure with antiferromagnetic layering appearing between adjacent sheets below $T_N \simeq 10$ K; the associated differences in lattice parameters are quite small, as $a = 3.555 \pm 0.006$ Å and $c = 7.537 \pm 0.010$ Å in HoNiBC while $a = 3.542 \pm 0.001$ Å and $c = 7.547 \pm 0.004$ Å in ErNiBC [4]. Furthermore, in GdNiBC [5], which displays a $c$-axis spacing ($\simeq$7.546 Å) very close to that reported above for the Er-substituted system (but with an $a$ value reduced

0953-8984/96/350483+08$19.50  

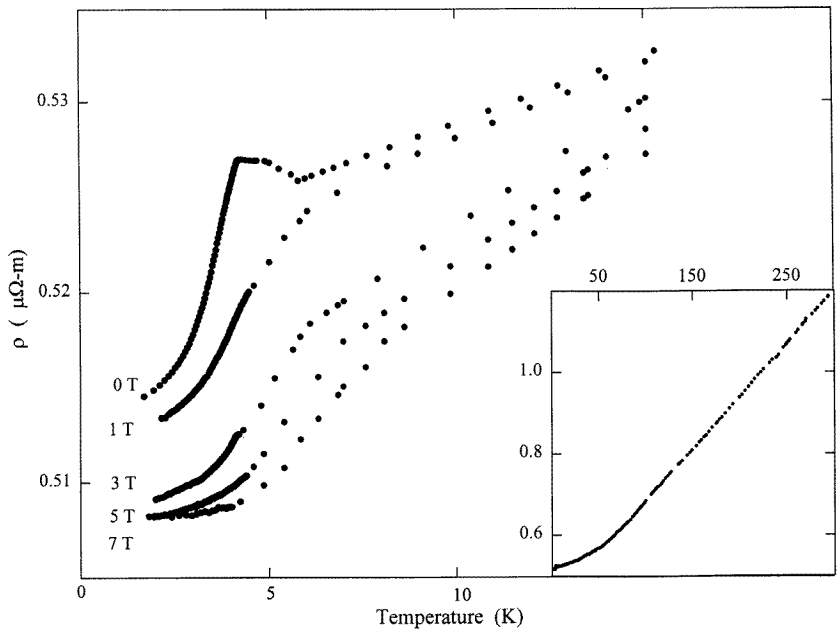


**Figure 1.** The temperature-dependent resistivity (in $\mu\Omega$ m) plotted against temperature (in K), between 1.5 and 15 K, in fixed fields of B = 0, 1, 3, 5 and 7 T. The inset shows the zero-field resistivity up to room temperature.

by some 0.011 Å), transport and magnetic data have been interpreted as indicating an antiferromagnetic ordering (of as yet undetermined structure) below $T_N \simeq 14$ K; these latter conclusions were based principally on the unusual resistivity–temperature behaviour of this system.

Here we report the results of a similar study of the resistivity, magnetoresistance and field-dependent AC susceptibility of ErNiBC; our conclusions are summarized below.

Standard arc melting techniques were used to prepare a sample from stoichiometric quantities of Er (>99.9%), Ni(99.95%), B (>99%) and specpure C; melting losses were negligibly small. To ensure homogeneity the resulting button was inverted and remelted four times, after which it was annealed in a (reduced) Ar atmosphere for 36 hours at 1000 °C followed by slow cooling. Finally, samples of approximate dimensions $(5 \times 0.9 \times 0.9)$ mm$^3$ suitable for transport and magnetic measurements were cut from it; details of the measuring techniques—a high-precision, low-frequency (37 Hz) differential method for measuring the resistivity and magnetoresistance [6] and a phase-locked susceptometer (operating at 2.4 kHz with a driving field of 5 $\mu$T rms) for evaluating the AC susceptibility [7]—have been presented previously.

X-ray measurements using Cu K$\alpha$ radiation on powder samples confirmed previous structural determinations and yielded $a \simeq 3.554$ Å and $c \simeq 7.574$ Å, which are slightly different from the values reported in [4], but intermediate, as expected, between values reported for LuNiBC ($a = 3.4985$ Å, $c = 7.7556$ Å [8]) and GdNiBC ($a = 3.631$ Å, $c = 7.546$ Å [5]); no significant impurity phases could be detected.

Figures 1, 2 and 3 summarize the principal results of this investigation. The inset in the first figure shows the general features of the zero-field resistivity; at room temperature

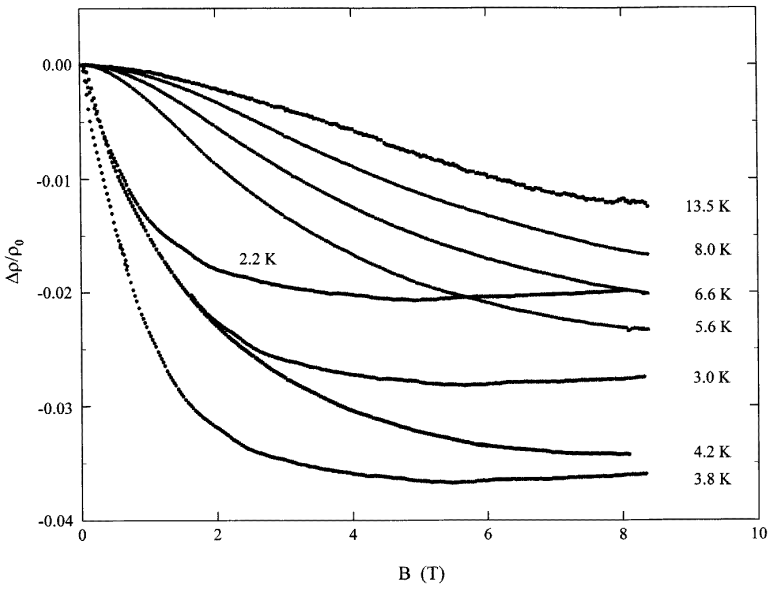


**Figure 2.** The fractional magnetoresistance $\Delta\rho/\rho_0$ ($= (\rho(0,\ T) - (\rho(B,\ T)/\rho(0,\ T))$ plotted against the applied field B (in T) at various fixed temperatures.

this resistivity $\rho$(300 K) is approximately 1.20 $\mu\Omega$ m (resistivity values are uncertain to typically $\pm 5\%$ due to shape factor and absolute AC voltage errors, although relative values can be measured to a few parts in $10^5$), close to the value reported for GdNiBC [5]. Below room temperature the system exhibits metallic behaviour, with $\mathrm{d}\rho/\mathrm{d}T \simeq 2.7$ n$\Omega$ m K$^{-1}$ (for $T \gtrsim 80$ K), again similar to that for GdNiBC. As shown in figure 1, $\rho(4.2\ \mathrm{K}) \simeq 0.527\ \mu\Omega$ m, some 30% less than that found for R = Gd [5], despite the effects of a significant reduction in spin-disorder scattering in this latter system at $T < T_N \simeq 14$ K; such differences can arise from various sources, including the presence of microcracks as well as differences in sample quality (an acute problem in these recently discovered borocarbides, as discussed below). The main body of figure 1 reproduces the resistivities $\rho$(B, T) measured between 1.4 and 15 K in *fixed* applied fields of 0, 1, 3, 5 and 7 T (these being oriented along the largest sample dimension). Apart from the small anomaly near 6 K (discussed below), these zero-field data increase gradually with increasing temperature above 6 K—usually attributed to phonon scattering effects—whereas below 5 K structure indicative of magnetic ordering is evident. Here an abrupt decrease in resistivity with decreasing temperature is observed, the onset of which appears near 4.4 K and below which $\rho$(0, T) falls monotonically; such behaviour is consistent with ferromagnetic ordering [9]. This sharp feature near $T_c$ is suppressed by increasing applied fields, so that in 7 T $\rho$(B, T) increases smoothly from 1.4 to 15 K. Figure 2 summarizes the magnetoresistivities, showing measurements at eight fixed temperatures between 2.2 and 13.5 K; these data support the conclusions reached above as the lower-field data vary approximately as $B^2$ for $T > T_c$ whereas below $T_c$ the low-field response is much more abrupt, as discussed later†. Figure 3 reproduces the field-dependent

† It should be noted that a strict comparison between the data in figures 1 and 2 is not appropriate due to field cooling/hysteretic effects; the data in figure 2 were all acquired in increasing field while those shown in figure 1 (below 4.2 K) were obtained in a fixed field as the temperature was lowered.

AC susceptibilities (measured in a fixed field, applied along the largest dimension, as a function of increasing temperature); the small anomaly near 6 K notwithstanding‡, the main effect of superimposed static biasing fields is to suppress the susceptibility generally, this suppression being most marked in the vicinity of the principal maximum evident in figure 3. In soft ferromagnetic systems this principal maximum is rapidly suppressed in both amplitude *and* temperature by such fields, an effect which facilitates the observations of (secondary) critical peaks [11]; the latter are also reduced in amplitude, but move *upward* in temperature with increasing field in a manner consistent with the predictions of the usual static scaling law equation of state [11, 12]. The field and temperature dependence of such critical peaks can be used to estimate the critical exponents $\gamma$, $\beta$ and $\delta$ [11, 13]. The failure to observe such structure here may be indicative of considerable 'technical' hardness; the technical or regular contribution to the total susceptibility arises from processes such as domain wall motion, coherent rotation, etc, which is not suppressed here in available applied fields. Systems in which these technical contributions are not suppressed in low field are termed 'technically hard' and as a consequence the contribution from critical fluctuations does not dominate the measured response. Here these effects are most likely to be attributable to single-ion anisotropy resulting from spin–orbit coupling at Er sites. The inset in figure 3 shows a butterfly loop taken at 4.2 K, indicating a coercive field of about 2 mT at that temperature (although not shown here, this field increases to beyond 10 mT at 1.7 K).

A detailed analysis of the zero-field resistivity data is summarized in figure 4, an analysis based on the identification of a ferromagnetic ground state from neutron diffraction measurements [4] as the present data do not preclude other forms of ordering. The dashed curve in this figure represents the derivative $\mathrm{d}\rho/\mathrm{d}T$ [14]; the extended plateau region in this derivative between about 3.5 and 4.1 K results from the linear decrease in $\rho_m(T)$ with decreasing temperature in this region, shown by a solid line. This linear variation is consistent with mean-field predictions for the magnetic resistivity in the temperature region immediately below $T_c$ accompanying ferromagnetic ordering ($\rho_m(T \lesssim T_c) \sim \langle J_z \rangle^2 \propto (T - T_c)^{2\beta}$; $\beta = 0.5$). Thus, identifying $T_c$ with the *upper* extension of this plateau yields $T_c = 4.13 \pm 0.05$ K. This latter estimate lies below the temperature at which a coercive field first appears, a result often associated with non-optimized sample quality [15],. The solid line at low temperatures in this figure is a fit of the magnetic resistivity $\rho_m(T)$ to these data using the form derived by Anderson and Smith [16] for the scattering of conduction electrons at low temperatures ($T \ll T_c$) by spin waves with a dispersion relation

$$E_q = \Delta + Dq^2 \tag{1}$$

where $D$ is the acoustic spin-wave stiffness, $q$ is the magnon wavevector and $\Delta$ is the gap in the spin-wave spectrum at $q = 0$ (the gapless forms, yielding $\rho_m \propto T^2$ (with wavevector conservation [17]) or $\rho_m \propto T^{3/2}$ (without wavevector conservation [18]), do *not* provide an adequate representation of the low-temperature data); this then leads to

$$\rho_m(T) = AT\Delta \mathrm{e}^{-\Delta/T}\left[1 + \frac{2T}{\Delta} + \frac{\mathrm{e}^{-\Delta/T}}{2} \cdots\right]. \tag{2}$$

‡ We are unable, at present, to indicate whether this feature is intrinsic to single-phase, stoichiometric ErNiBC; a similar feature is evident in previous measurements of the zero-field AC susceptibility of this system (figure 1 of [4]), although there it appeared at a higher temperature. The combined behaviour shown in figures 1 and 3 rules out a Kondo effect associated with Er moments (at or slightly away from stoichiometry) and possible $ErNi_2B_2C$ superconducting inclusions (at levels below that detectable by x-rays). This feature is, however, close to the (coexistent) antiferromagnetic transition temperature for $ErNi_2B_2C$ [10].

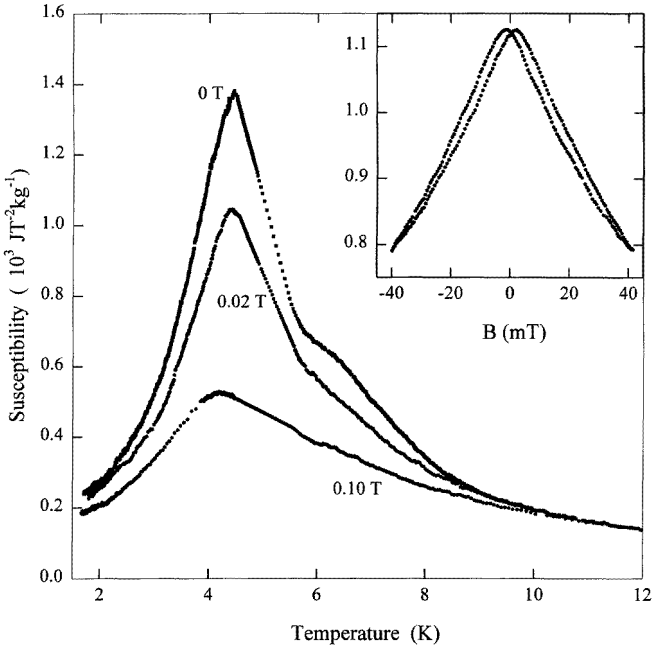


**Figure 3.** The AC susceptibility (in J T$^{-2}$ kg$^{-1}$) plotted against temperature (in K) in three fixed, static biasing fields. The inset shows a butterfly loop at 4.2 K which enables the coercive field to be estimated.

The value deduced for the gap parameter is $\Delta = 2 \pm 0.5$ K; this estimate is based on a least-squares fitting routine and is quite sensitive to both the temperature interval chosen and the number of terms retained in (2). The value shown for $\Delta$ utilizes all three terms shown in this latter equation (along with an adjustable residual term $\rho_0$) and covers the temperature interval from 1.5 K to a variable upper temperature cut-off from 1.9 to 2.3 K. The listed uncertainty in $\Delta$ is determined by the variation observed over these ranges; in this regard it is important to point out that in no case does the least-squares regression coefficient fall below 0.998, and the $\Delta$ values do *not* shift monotonically as the upper fitting temperature is reduced. This is in spite of the fact that this latter temperature represents a significant fraction of $T_c$ (clearly more data in the temperature interval below the pumped $He^4$ range currently available to us would help in this respect). Changes in $\Delta$ are accompanied by changes in the coefficient $A$; we find $A = 0.025 \mp 0.008$ (with the product $A\Delta$ being $0.05 \pm 0.01$ (3)). Increasing the upper temperature cut-off beyond 2.3 K causes $\Delta$ to increase rapidly with an associated marked deterioration in the fit to the lowest-temperature data, data to which the asymptotic form shown in (2) should be most appropriate. Fitting just the first term in (2) over the same temperature range(s) gives $\Delta = 3.2 \pm 0.6$ K.

The overall change in the magnetic resistivity $\Delta\rho_m$ between $T_c$ and $T = 0$ allows an estimate for the local Er moment–conduction electron exchange coupling constant $\Gamma$ in the s-f model [18] to be made; in this model the scattering potential at the Er sites is described by

$$\mathcal{H}_{sf} = V - 2\Gamma(g_J - 1)\boldsymbol{J} \cdot \boldsymbol{s} \tag{3}$$

where $V$ is the screened Coulomb potential, $\boldsymbol{J}$ is the total Er angular momentum and $\boldsymbol{s}$ is

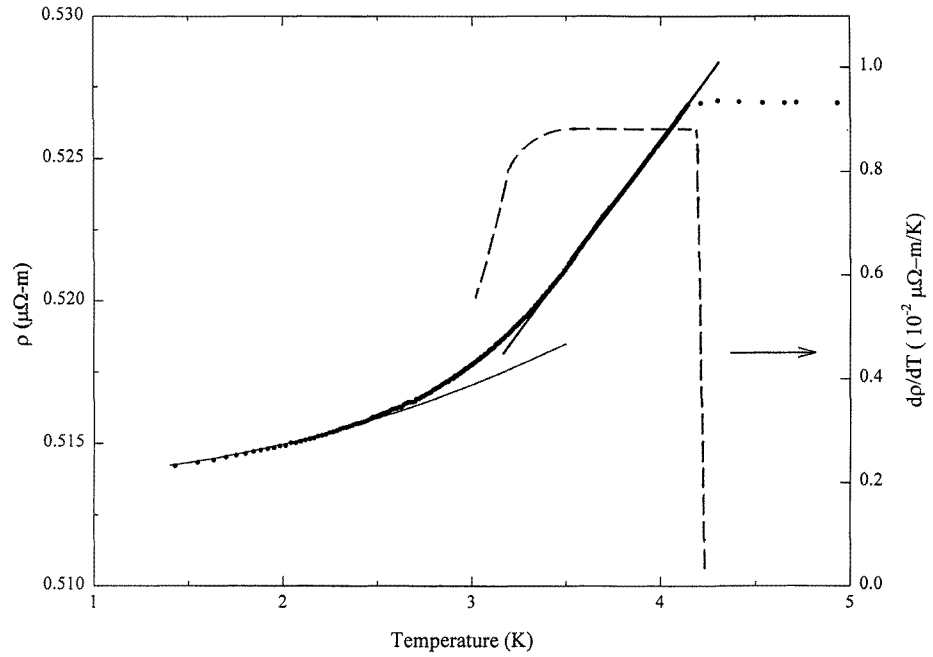


**Figure 4.** The zero-field resistivity (in $\mu\Omega$ m) plotted against temperature (in K) below 5 K. The dashed line represents the derivative $\mathrm{d}\rho/\mathrm{d}T$ (in $\mu\Omega$ m $\mathrm{K}^{-1}$). The solid line through the lowest-temperature data represents a fit to (2), while the solid line through the data immediately below $T_c$ illustrates the mean-field prediction for ferromagnetic ordering.

the conduction electron spin.

For ferromagnetic ordering, this approach yields

$$\Delta\rho_m \approx C\left(g_J - 1\right)^2 \Gamma^2 J(1+4J) \qquad V^2 \gg \Gamma^2 \tag{4}$$

in which

$$C = \frac{3\pi m^*}{2\hbar e^2 E_F} c\left(\frac{V}{N}\right) \tag{5}$$

incorporates the band structure details; with $m^*$ taken as the free electron mass, $c$ the atomic fraction of Er, is 0.25, $V/N$, the unit cell volume divided by the number of atoms in that volume, is approximately 12 Å$^3$ [8] and the Fermi velocity $v_F = 2 \times 10^5$ m $\mathrm{s}^{-1}$ (the value derived for $LuNi_2B_2C$ [19] scaled by the estimated valence electron concentration ratio between $LuNi_2B_2C$ and LuNiBC [8, 20]); then $C \simeq 7.2$ $\mu\Omega$ m $\mathrm{eV}^{-2}$. Neglecting crystal field effects [20] yields $(g_J - 1)^2 J(1+4J) \simeq 9$, from which one finds an admittedly approximate value for $|\Gamma|$ of 15 meV; the same model approach applied to the linear decrease in $\rho_m(T)$ evident immediately below $T_c$ yields $|\Gamma| \simeq 20$ meV.

Figure 5 reproduces the field-dependent resistivities, measured in fixed fields of 1, 3, 5 and 7 T, in the temperature region below 4 K. The solid lines in this figure represent the predictions of (1) and (2) in a field, when

$$\Delta \rightarrow \Delta + g_J \mu_B B. \tag{6}$$

With crystal field effects neglected, $g_J = 6/5$, and these solid lines utilize the same range of $\Delta$ and $A$ values found from the zero-field data. These fits provide an adequate fit to

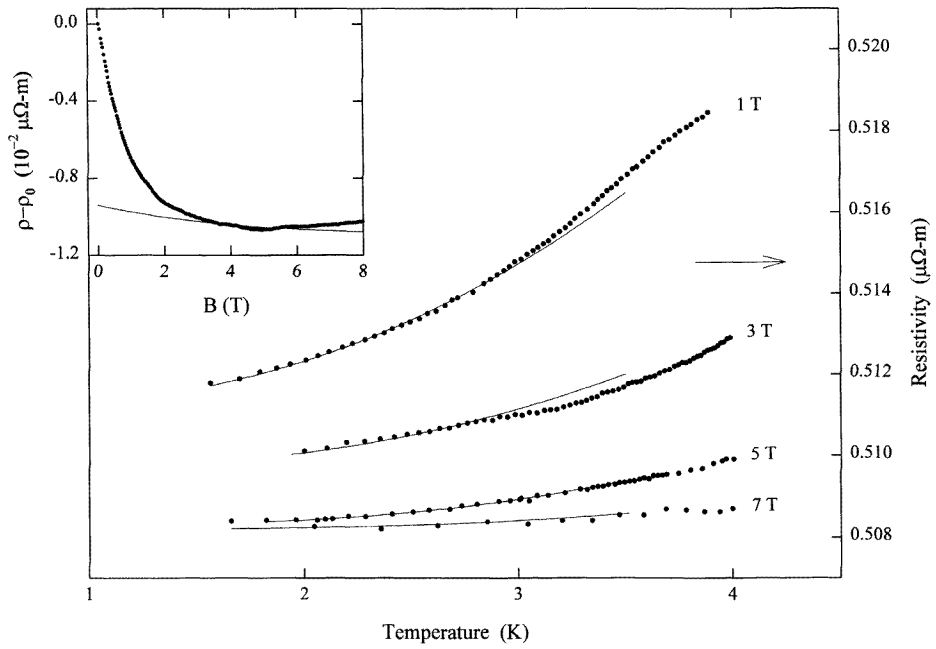


**Figure 5.** The resistivity (in $\mu\Omega$ m) plotted against temperature (in K) below 4 K, in fixed fields of $B = 1$, 3, 5 and 7 T. The solid lines represent fits to (2) with a Zeeman term added to the gap $\Delta$. The inset shows the magnetoresistance at 2.2 K compared with its predicted dependence (solid line).

these data (although measurements extending below the pumped $He^4$ range would also be useful here), from which we conclude that the temperature dependences of the zero-field and of the fixed-field resistivities are consistent with spin-wave scattering well below $T_c$ with a conventional field-induced modification of the gap parameter.

One aspect of the behaviour of the magnetoresistance is, however, anomalous: not its temperature dependence, fitted as discussed above, but the marked field dependence of the 'residual' resistivity term, $\rho_0(B,\ T \ll T_c)$, evident on close inspection of figures 2 and 5. The decrease in $\rho_0(B,\ T \ll T_c)$ between 0 and 7 T is far larger than expected. This point is made explicitly in the inset of figure 5 in which the field-induced change in the resistivity at 2.2 K is shown. The solid line in this figure reproduces the predictions of (2) incorporating the modification of $\Delta$ by an applied field (6). The offset evident at zero applied field in this inset between the calculated response and its measured value (some 9 n$\Omega$ m) is a measure of this anomalous decrease. As far as the origin of this effect is concerned, we note that its magnitude is somewhat larger than, but not inconsistent with, the anomaly evident in the zero-field data near 6 K. This anomaly is suppressed by all fixed fields used in this investigation (and indeed it does not appear to contribute to the temperature dependence of the data shown in figure 5), and we suggest therefore that it is the likely cause of the unusually large variation inferred for $\rho_0(B,\ T \ll T_c)$.

In summary, the temperature (1.5–15 K) and field-dependent (0–7 T) resistivities of ErNiBC are consistent with the onset of ferromagnetic order below $T_c \simeq 4.13$ K and with conduction electron–spin wave scattering (well below $T_c$), the latter being described by a gap parameter $\Delta \simeq 2 \pm 0.5$ K. Ferromagnetic critical fluctuations are not observed in the

field-dependent AC susceptibility due, possibly, to magnetic anisotropy/technical hardness attributable to spin–orbit coupling at the Er sites. Finally, it should be noted that the present data do not identify the ground state spin configuration unambiguously—equation (2) has been used to fit the resistivity of antiferromagnetic $URu_2Si_2$ [21]—unlike the definitive conclusion inferred from neutron data.

We thank B W Southern for discussions, P A Stampe for assistance with the computer fits and INCO (Canada) for providing the pure Ni used in this investigation. This work was supported in part by grants from the Natural Sciences and Engineering Research Council of Canada.

## References

[1] Cava R J, Takagi H, Zandbergen H W, Krajewski J J, Peck W F Jr, Siegrist T, Batlogg B, van Dover R B, Felder R J, Mizuhashi K, Lee J O, Eisaki H and Uchida S 1994 *Nature* **367** 252

[2] Eisaki H, Takagi H, Cava R J, Batlogg B, Krajewski J J, Peck W F Jr, Mizuhashi K, Lee J O and Uchida S 1994 *Phys. Rev.* B **50** 647

[3] Hill J P, Sternlieb B J, Gibbs D, Detlefs C, Goldman A I, Stassis C, Canfield P C and Cho B K 1996 *Phys. Rev.* B **53** 3487
Zarestky J, Stassis C, Goldman A I, Canfield P C, Der Venagas D, Cho B K and Johnston D C 1995 *Phys. Rev.* B **51** 678
Shina S K, Lynn J W, Grigereit T E, Hossain Z, Gupta L C, Nagarajan R and Godart C 1995 *Phys. Rev.* B **51** 681

[4] Chang L J, Tomy C V, Paul D McK, Anderson N H and Yethirja M !996 *J. Phys.: Condens. Matter* **8** 2119; the lattice parameter estimates were included in the preprint version of this paper, not the published version.

[5] El Massalami M, Giordanengo B, Mondragon J, Baggio-Saitovitch E M, Takeuchi A, Voiron J and Sulpice A 1995 *J. Phys.: Condens. Matter* **7** 10 015

[6] Muir W B and Ström-Olsen J O 1976 *J. Phys. E: Sci. Instrum.* **9** 163

[7] Wang Z, Kunkel H P and Williams Gwyn 1992 *J. Phys.: Condens. Matter* **4** 10 385

[8] Siegrist T, Zandbergen H W, Cava R J, Krajewski J J and Peck W F Jr 1995 *Nature* **367** 254

[9] Mydosh J A, Budnick J I, Kawatra M P and Skalski S 1968 *Phys. Rev. Lett.* **21** 1346
Kawatra M P and Budnick J I 1970 *Int. J. Mag.* **1** 61

[10] Cho B K, Canfield P C, Miller L L, Johnston D C, Beyerman W P and Yatskar A 1995 *Phys. Rev.* B **52** 3684

[11] Williams Gwyn 1991 *Magnetic Susceptibility of Superconductors and other Spin Systems* ed R A Hein *et al* (New York: Plenum) p 475

[12] Stanley H E 1971 *Introduction to Phase Transition and Critical Phenomena* ed T L Francavilla and D H Liebenberg (Oxford: Clarendon)

[13] Contrast the behaviour reported, for example, in [7] with that in Wang Z, Kunkel H P and Williams G 1990 *J. Phys.: Condens. Matter* **2** 4173.

[14] These derivatives were found in general by fitting the experimental data to an arbitrary 'best fit' analytic expression which was subsequently differentiated; the plateau region corresponds to the fit of the region between 3.5 and 4.1 K by a straight line.

[15] Rastogi A K and Coles B R 1986 *J. Magn. Magn. Mater.* **54–7** 117

[16] Anderson N H and Smith H 1979 *Phys. Rev.* B **19** 384

[17] Kasuya T 1959 *Prog. Theor. Phys.* **22** 227
Mannari I 1959 *Prog. Theor. Phys.* **22** 335
Goodings D 1963 *Phys. Rev.* **132** 542

[18] Long P D and Turner R E 1970 *J. Phys. C: Solid State Phys.* **3** S127
Yosida K 1957 *Phys. Rev.* **107** 396

[19] Pickett W E and Singh D J 1994 *Phys. Rev. Lett.* **72** 3702

[20] Mattheiss L F 1994 *Phys. Rev.* B **49** 13 279
Kim H, Hwang C-D and Ihm J 1995 *Phys. Rev.* B **52** 4592

[21] Mentink S A M, Mason T E, Süllow S, Nieuwenhuys G J, Menovsky A A, Mydosh J A and Perenboom J A A J 1996 *Phys. Rev.* B **53** R6014